Voltage Generation by Ferromagnetic Resonance at a Nonmagnet to Ferromagnet Contact

Xuhui Wang,[1] Gerrit E. W. Bauer,[1] Bart J. van Wees,[2] Arne Brataas,[3] and Yaroslav Tserkovnyak[4]

[1]*Kavli Institute of NanoScience, Delft University of Technology, 2628 CJ Delft, The Netherlands*
[2]*Department of Applied Physics and Materials Science Center, University of Groningen, Nijenborgh 4, 9747 AG Groningen, The Netherlands*
[3]*Department of Physics, Norwegian University of Science and Technology, N-7491 Trondheim, Norway*
[4]*Lyman Laboratory of Physics, Harvard University, Cambridge, Massachusetts 02138, USA, and Department of Physics and Astronomy, University of California, Los Angeles, California 90095, USA*

(Received 1 August 2006; published 22 November 2006)

A ferromagnet can resonantly absorb rf radiation to sustain a steady precession of the magnetization around an internal or applied magnetic field. We show that, under these ferromagnetic resonance conditions, a dc voltage is generated at a normal-metal electric contact to a ferromagnet with spin-flip scattering. The spin dynamics in the nonmagnetic region is accounted for by a frequency-dependent renormalization of the interface conductances. This mechanism allows sensing of time-dependent magnetizations by established dc electronic techniques.

DOI: 10.1103/PhysRevLett.97.216602 PACS numbers: 76.50.+g, 72.25.Mk, 73.23.−b, 73.40.−c

The field of magnetoelectronics utilizes the electronic spin degrees of freedom to achieve new functionalities in circuits and devices made from ferromagnetic and normal conductors. The modulation of the dc electrical resistance by means of the relative orientation of the magnetizations of individual ferromagnetic elements (''giant magnetoresistance'') is by now well established. Dynamic effects, such as the current-induced magnetization reversal, are still a subject of cutting edge research activities. Here we concentrate on an application of the concept of spin pumping, i.e., the emission of a spin current from a moving magnetization of a ferromagnet (F) in electrical contact with a normal conductor (N) [1,2], viz., the ''spin battery'' [3]. In this device, a ferromagnet that precesses under ferromagnetic resonance (FMR) conditions pumps a spin current into an attached normal metal that may serve as a source of a constant spin accumulation (see also Ref. [4]). In this Letter, we report that spin-flip scattering in the ferromagnet translates the pumped spin accumulation into a charge voltage over an $F|N$ junction. Because of the spin-flip scattering in F, a backflow spin current collinear to the magnetization is partially absorbed in the ferromagnet. Since the interface and bulk conductances are spin-dependent, this leads to a net charging of the ferromagnet, which thus serves as a source as well as electric analyzer of the spin-pumping current. We note the analogy to the voltage in excited $F|N|F$ spin valves predicted by Berger [5] and recently analyzed by Kupferschmidt *et al.* [6]. Since the spin-flip scattering in conventional magnets such as permalloy (Py) is very strong, this effect provides a handle to experimentally identify the FMR-induced spin accumulation in the simplest setup [7]. A detailed experimental test of our predictions is in progress [8].

The spin battery operated by ferromagnetic resonance has been proposed by Brataas *et al.* [3] in the limit of weak spin-flip scattering in the ferromagnet. It is based on the spin current pumped into a normal metal by a moving magnetization ($F|N$) [1]

$$\mathbf{I}_s^{(p)} = \frac{\hbar}{4\pi}\left(\mathrm{Re}g^{\uparrow\downarrow}\mathbf{m}\times\frac{d\mathbf{m}}{dt} + \mathrm{Im}g^{\uparrow\downarrow}\frac{d\mathbf{m}}{dt}\right), \tag{1}$$

where $\mathbf{m}$ is the unit vector of magnetization. $\mathrm{Re}g^{\uparrow\downarrow}$ and $\mathrm{Im}g^{\uparrow\downarrow}$ are the real and imaginary parts, respectively, of the (dimensionless) spin-mixing conductance $g^{\uparrow\downarrow}$ [9]. This spin current creates a spin accumulation $\mathbf{s}$ in the normal metal, which induces a backflow of spins and, as we will see, charges the ferromagnet. According to magnetoelectronic circuit theory [9], the charge and spin currents flowing through the $F|N$ interface (into N) in the presence of nonequilibrium charge and spin accumulations μ_0^N, $\mathbf{s}$ in N and μ_0^F, $\mu_s^F\mathbf{m}$ in F read [9]

$$\begin{aligned} I_c &= \frac{eg}{2h}[2(\mu_0^F-\mu_0^N) + p\mu_s^F - p(\mathbf{m}\cdot\mathbf{s})], \\ \mathbf{I}_s^{(b)} &= \frac{g}{8\pi}[2p(\mu_0^F-\mu_0^N) + \mu_s^F - (1-2\mathrm{Re}g^{\uparrow\downarrow}/g)\mathbf{m}\cdot\mathbf{s}]\mathbf{m} \\ &\quad -\frac{\mathrm{Re}g^{\uparrow\downarrow}}{4\pi}\mathbf{s} - \frac{\mathrm{Im}g^{\uparrow\downarrow}}{4\pi}(\mathbf{s}\times\mathbf{m}), \end{aligned} \tag{2}$$

where $g = g^{\uparrow} + g^{\downarrow}$ is the total interface conductance of spin-up and spin-down electrons, and p is the contact polarization given by $p = (g^{\uparrow} - g^{\downarrow})/(g^{\uparrow} + g^{\downarrow})$. For typical metallic interfaces, the imaginary part of the mixing conductance is quite small [10] and, hence, is discarded in the following discussion. We choose the transport direction along the x axis that is perpendicular to the interface at the origin. $\mathbf{H}_{\mathrm{ex}}$, the sum of dc external and uniaxial anisotropy magnetic fields, points in the z direction, which is also the chosen spin quantization axis in the normal metal. At the ferromagnetic resonance, the magnetization precesses steadily around the z axis with azimuthal angle θ (see Fig. 1) that is tunable by the intensity of an ac magnetic field. The thickness of the normal and ferromagnetic metal films are d_N and d_F, respectively. $\mathbf{s}(x, t)$ is determined by

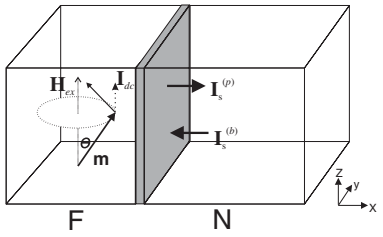

FIG. 1. Schematic view of a spin battery operated by ferromagnetic resonance. The dotted line $\mathbf{I}_{\rm dc}$ represents the dc component of the pumping current.

the spin-diffusion equation [11]

$$\frac{\partial \mathbf{s}}{\partial t} = D_N \frac{\partial^2 \mathbf{s}}{\partial x^2} - \frac{\mathbf{s}}{\tau_{\rm sf}^N}, \tag{3}$$

where $\tau_{\rm sf}^N$ is the spin-flip relaxation time and D_N the diffusion constant in the normal metal. Assuming that the magnetization precesses around the z axis with angular velocity ω, we consider the limit where the spin-diffusion length in the normal metal is much larger than the transverse spin-averaging length $l_\omega \equiv \sqrt{D_N/\omega}$, i.e., $\lambda_{\rm sd}^N = \sqrt{D^N/\tau_{\rm sf}} \gg l_\omega$, or equivalently $\omega\tau_{\rm sf}^N \gg 1$. We can then distinguish two regimes. When the thickness of the normal metal $d_N \gg l_\omega$, which is equivalent to the Thouless energy $\hbar D_N/d_N^2 \ll \hbar\omega$, the oscillating transverse component of the induced spin accumulation vanishes inside most of the normal metal, and one is left with a time-independent spin accumulation along the z axis decaying away from the interface on the scale $\lambda_{\rm sd}^N$. The backflow due to the steady state spin accumulation aligned along the z axis cancels the same component of the pumping current. The former acquires the universal value $\hbar\omega$ when the spin-flip scattering is sufficiently weak [3]. In the opposite regime of ultrathin normal-metal films with $\hbar D_N/d_N^2 \gg \hbar\omega$, the spin accumulation $\mathbf{s}$ is governed by a Bloch equation and will be discussed elsewhere [12].

Continuity of the total spin current into the normal metal at the interface

$$\mathbf{I}_s = \mathbf{I}_s^{(p)} + \mathbf{I}_s^{(b)} \tag{4}$$

is the first boundary condition for the diffusion equation: $\partial\mathbf{s}/\partial x|_{x=0} = -2\mathbf{I}_s/(\hbar\nu_{\rm DOS}AD_N)$, where $\nu_{\rm DOS}$ is the one-spin density of states and A the area of the interface. We also require vanishing of the spin current at the outer boundary $\partial\mathbf{s}/\partial x|_{x=d_N} = 0$. The time-averaged solution of Eq. (3) reads $\langle\mathbf{s}\rangle_t = s_z\hat{\mathbf{z}}$, with

$$s_z = \frac{\cosh(x-d_N)/\lambda_{\rm sd}^N}{\sinh d_N/\lambda_{\rm sd}^N} \frac{2\lambda_{\rm sd}^N}{\hbar\nu_{\rm DOS}AD_N} I_{s,z}. \tag{5}$$

The component of the spin accumulation parallel to the magnetization is a constant for the precessional motion considered here. It can penetrate the ferromagnet, hence building up a spin accumulation $\mu_s^F = \mu_\uparrow^F - \mu_\downarrow^F$ in F, which obeys the spin-diffusion equation [11]

$$\frac{\partial^2\mu_s^F(x)}{\partial x^2} = \frac{\mu_s^F(x)}{(\lambda_{\rm sd}^F)^2}, \tag{6}$$

where $\lambda_{\rm sd}^F$ is the spin-flip diffusion length in the ferromagnet. The boundary conditions are given by the continuity of the longitudinal spin current at the interface

$$\sigma_\uparrow\left(\frac{\partial\mu_\uparrow^F}{\partial x}\right)_{x=0} - \sigma_\downarrow\left(\frac{\partial\mu_\downarrow^F}{\partial x}\right)_{x=0} = -\frac{2e^2}{\hbar A} I_{s,z}\cos\theta \tag{7}$$

and a vanishing spin current at the outer boundary

$$\sigma_\uparrow\left(\frac{\partial\mu_\uparrow^F}{\partial x}\right)_{x=-d_F} - \sigma_\downarrow\left(\frac{\partial\mu_\downarrow^F}{\partial x}\right)_{x=-d_F} = 0, \tag{8}$$

where $\sigma_{\uparrow(\downarrow)}$ is the conductivity of spin-up (-down) electrons in the ferromagnet. In the steady state, there can be no net charge flow. From $I_c = 0$ follows that a charge chemical potential difference $\mu_0^F - \mu_0^N = p[s_z\cos\theta - \mu_s^F]_{x=0}/2$ builds up across the contact. At the interface on the F side, the longitudinal component of the total spin current leaving the ferromagnet then reads

$$I_{s,z}\cos\theta = \frac{(1-p^2)g}{8\pi}[\mu_s^F - s_z\cos\theta]_{x=0}. \tag{9}$$

The interface resistance is in series with a resistance $\rho_\omega = l_\omega/(h\nu_{\rm DOS}AD_N)$ of the bulk normal metal of thickness l_ω that accounts for the averaging of the transverse spin current components. This reduces the interface conductances for spin-up (-down) electrons to $g_\omega^{\uparrow(\downarrow)} = g^{\uparrow(\downarrow)}/(1+\rho_\omega g^{\uparrow(\downarrow)})$ and the spin-mixing conductance $g_\omega^{\uparrow\downarrow} = {\rm Re}g^{\uparrow\downarrow}/(1+\rho_\omega\,{\rm Re}g^{\uparrow\downarrow})$. We also introduce

$$g_\omega = g_\omega^\uparrow + g_\omega^\downarrow, \qquad p_\omega = \frac{g_\omega^\uparrow - g_\omega^\downarrow}{g_\omega^\uparrow + g_\omega^\downarrow}. \tag{10}$$

Solving Eq. (6) under the above boundary conditions gives

$$\mu_s^F(x) = \frac{\tilde{g}\cosh[(x+d_F)/\lambda_{\rm sd}^F]\cos\theta}{[\tilde{g} + g_F\tanh(d_F/\lambda_{\rm sd}^F)]\cosh(d_F/\lambda_{\rm sd}^F)} s_z|_{x=0}, \tag{11}$$

where $\tilde{g} = (1-p_\omega^2)g_\omega$ and $g_F = 4hA\sigma_\uparrow\sigma_\downarrow/[e^2\lambda_{\rm sd}^F(\sigma_\uparrow + \sigma_\downarrow)]$ parametrizes the properties of the bulk ferromagnet [13]. When the spin-flip in F is negligible, i.e., $d_F \ll \lambda_{\rm sd}^F$, then $\mu_s^F|_{x=0} = s_z|_{x=0}\cos\theta$, and, consequently, the longitudinal spin current vanishes. In the present limit $\omega\tau_{\rm sf}^N \gg 1$, the time-averaged pumping current Eq. (4) reads $I_{s,z}^{(p)} = \hbar\omega\,{\rm Re}g^{\uparrow\downarrow}\sin^2\theta/4\pi$, and the spin accumulation in N at distance l_ω near the interface becomes

$$s_z = \frac{\hbar\omega\sin^2\theta}{\eta_N + \sin^2\theta + \frac{(1-p_\omega^2)\eta_F^{\uparrow\downarrow}}{1-p_\omega^2+\eta_F}\cos^2\theta}, \tag{12}$$

where we have introduced the reduction factors for N and F:

$$\eta_N = \frac{g_N}{g_\omega^{\uparrow\downarrow}} \tanh\frac{d_N}{\lambda_{\rm sd}^N}, \qquad \eta_F^{\uparrow\downarrow} = \frac{g_F}{g_\omega^{\uparrow\downarrow}} \tanh\frac{d_F}{\lambda_{\rm sd}^F}, \tag{13}$$

where $g_N = h\nu_{\rm DOS}AD_N/\lambda_{\rm sd}^N$ and $\eta_F = g_\omega^{\uparrow\downarrow}\eta_F^{\uparrow\downarrow}/g_\omega$. With weak spin flip in F, i.e., $d_F \ll \lambda_{\rm sd}^F$, $\eta_F^{\uparrow\downarrow} \approx 0$ and Eq. (12) reduces to $s_z = \hbar\omega\sin^2\theta/[\eta_N + \sin^2\theta]$ [3]. Increasing the spin flip in F or the ratio $d_F/\lambda_{\rm sd}^F$, the factor $\eta_F^{\uparrow\downarrow}$ gets larger and the spin accumulation signal decreases accordingly. More interesting is the chemical potential bias $\Delta\mu_0 = \mu_0^F - \mu_0^N$ that builds up across the interface, for which we find

$$\Delta\mu_0 = \frac{\hbar\omega p_\omega(\eta_F/2)\sin^2\theta\cos\theta}{\alpha_F[\eta_N(\omega) + \sin^2\theta] + (1 - p_\omega^2)\eta_F^{\uparrow\downarrow}\cos^2\theta}, \tag{14}$$

where $\alpha_F = 1 - p_\omega^2 + \eta_F$. We now estimate the magnitude of s_z and $\Delta\mu_0$ for the typical systems Py|Al [14]. In Al, the spin-diffusion length is $\lambda_{\rm sd}^N = 500$ nm, the spin-flip time $\tau_{\rm sf}^N = 100$ ps (at low temperature), and the density of states of Al is $\nu_{\rm DOS} = 1.5 \times 10^{47}\ {\rm J}^{-1}\,{\rm m}^{-3}$. The mixing conductance of the Py|Al interface in a diffuse environment can be estimated as twice the Sharvin conductance of Al [15] to be ${\rm Re}g_{\uparrow\downarrow}/A \approx 20 \times 10^{19}\ {\rm m}^{-2}$. The bare contact polarization is taken as $p = 0.4$. The spin-flip length in Py is very short, around $\lambda_{\rm sf}^F = 5$ nm [16], and $(\sigma_\uparrow + \sigma_\downarrow)/\sigma_\uparrow\sigma_\downarrow$ is about $6.36 \times 10^{-7}\ \Omega\,{\rm m}$ [17]. Assuming a magnetization precession cone of $\theta = 5°$, the voltage $\Delta\mu_0/e$ of Py|Al interface as a function of the FMR frequency is plotted in Fig. 2. The induced spin accumulation in the normal metal and the voltages across the interface as a function of d_F are plotted in Fig. 3. The voltage bias across the interface, for given bulk properties of the normal metal, is seen to saturate at large spin-flip scatterings on the F side $d_F \gg \lambda_{\rm sd}^F$. Spin flip in the normal metal is detrimental to both spin accumulation and voltage generation. On the other hand, a transparency of the contact reduced from the Sharvin value increases the polarization p_ω up to its bare interface value and with it the voltage signal (up to a maximum value governed by the reduction factor η_N that wins in the limit of very low transparency).

The angle dependence of the voltage across the interface is plotted in the inset in Fig. 2 in the limit of large spin flip in F $d_F \gg \lambda_{\rm sd}^F$. When $d_N \ll \lambda_{\rm sd}^N$ (but still $d_N \gg l_\omega$), we obtain the maximum value:

$$\Delta\mu_0 = \frac{\hbar\omega p_\omega(g_F/2g_\omega)\sin^2\theta\cos\theta}{\alpha_F\sin^2\theta + (1 - p_\omega^2)g_F\cos^2\theta/g_\omega^{\uparrow\downarrow}}, \tag{15}$$

given $\alpha_F \to 1 - p_\omega^2 + g_F/g_\omega$. At a small angle of the magnetization precession θ,

$$\Delta\mu_0 = \frac{p_\omega g_\omega^{\uparrow\downarrow}\theta^2}{2(1 - p_\omega^2)g_\omega}\hbar\omega, \qquad \theta \to 0. \tag{16}$$

In the opposite limit $d_N \gg \lambda_{\rm sd}^N$ (but $\lambda_{\rm sd}^N \gg l_\omega$), the voltage drop becomes

$$\Delta\mu_0 = \frac{\hbar\omega p_\omega(g_F/2g_\omega)\sin^2\theta\cos\theta}{\alpha_F(g_N/g_\omega^{\uparrow\downarrow} + \sin^2\theta) + (1 - p_\omega^2)g_F\cos^2\theta/g_\omega^{\uparrow\downarrow}}, \tag{17}$$

which in the limit of a small angle reduces to

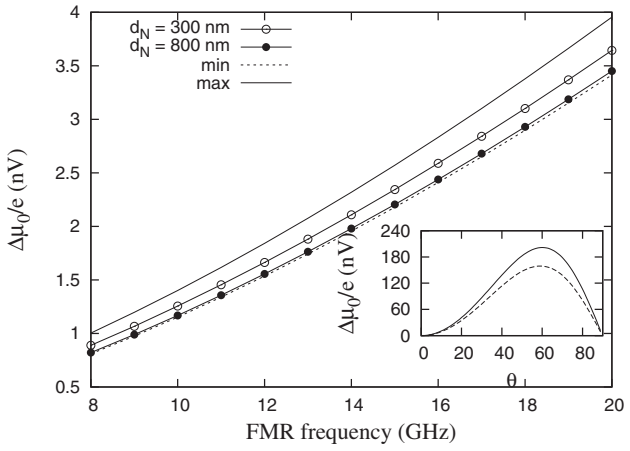

FIG. 2. The voltage drop $\Delta\mu_0/e$ (in units of nV) as a function of FMR frequency (in GHz) for the Py|Al interface. The line with circles denotes the situations when $d_N = 300$ nm (empty symbols) and $d_N = 800$ nm (solid symbols), where the thickness of ferromagnet is $d_F = 14$ nm. The solid and dashed lines refer to the limits as indicated by Eqs. (15) and (17), respectively. These curves indicate that, due to averaging of the transverse spin components inside the normal metal, the voltage is not linear with FMR frequency. The precession angle of magnetization is taken as $\theta = 5°$. The inset shows the angle dependence of the voltage at fixed frequency 15.5 GHz. At a small angle, the voltage drop is proportional to θ^2.

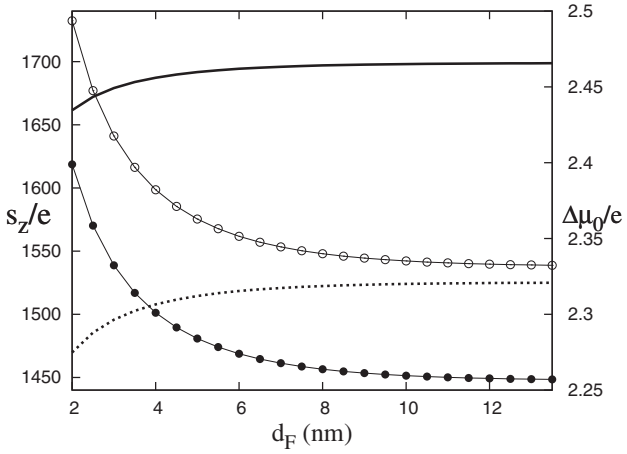

FIG. 3. Lines with circles are the spin-pumping-induced accumulation s_z/e (in units of nV) in Al near the interface to permalloy as a function of the Py layer thickness d_F and two Al layer thicknesses, i.e., $d_N = 300$ nm (empty symbols) and $d_N = 800$ nm (solid symbols). Solid ($d_N = 300$ nm) and dotted ($d_N = 800$ nm) lines are the chemical potential discontinuity across the interface $\Delta\mu_0/e$ (in units of nV), as a function of the Py layer thickness d_F. The FMR frequency is 15.5 GHz.

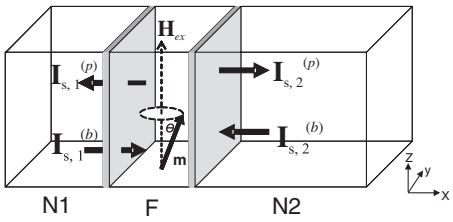

FIG. 4. The $N1|F|N2$ system in which the sandwiched F layer precesses around the z axis under the FMR condition. The origin of the x axis is located at the $F|N_2$ interface.

$\Delta\mu_0 \rightarrow p_\omega g_\omega^{\uparrow\downarrow}\theta^2\hbar\omega/[2(1+g_N/g_F)(1-p_\omega^2)g_\omega + 2g_N]$. In both limits at small precession angles, the voltages are proportional to θ^2, i.e., increase linearly with power intensity of the ac field. Equations (15) and (17) as a function of FMR frequency are depicted in Fig. 2 as solid and dashed lines, respectively.

In contrast to Berger [5], who predicted voltage generation in spin valves, viz., that dynamics of one ferromagnet causes a voltage when analyzed by a second ferromagnet through a normal-metal spacer, we consider here a simple bilayer. The single ferromagnetic layer serves simultaneously as a source and detector of the spin accumulation in the normal-metal layer. The presence of spin-flip scattering that allows the backflow of a parallel spin current is essential, and permalloy is ideal for this purpose. The voltage bias under FMR conditions can be measured simply by separate electrical contacts to the F and N layers. It can be detected even on a single ferromagnetic film with normal-metal contacts [7], provided that the two contacts are not equivalent.

We can also study the FMR-generated bias in a controlled way in the $N1|F|N2$ trilayers in which the F layer is sandwiched by two normal-metal layers (Fig. 4). The magnetization of the ferromagnet again precesses around the z axis. The thicknesses of $N1$, F, and $N2$ in the transport direction are d_{N1}, d_F, and d_{N2}, respectively. The spin-diffusion length in normal-metal node i is λ_i. With weak spin flip in the sandwiched ferromagnetic layer $d_F \ll \lambda_{\rm sd}^F$, the spin accumulation of F at both interfaces is the same. We find that the values of μ_s^F near the interfaces are mixtures of the interface values of the spin accumulations in the normal metals. In other words, the two normal metals talk to each other through F by the backflow and the generated voltages across the interfaces are different given different contacts. In the opposite limit with massive spin flip in F, $d_F \gg \lambda_{\rm sd}^F$, the strong spin-flip scattering eventually separates the spin accumulation in the two normal-metal nodes such that the "exchange" between the two normal metals is suppressed. We then recover Eq. (11).

According to Eq. (14), the voltage drops across the interfaces $\Delta\mu_0^{(1)} \equiv \mu_0^F - \mu_0^{N1}$ and $\Delta\mu_0^{(2)} \equiv \mu_0^F - \mu_0^{N2}$ are different for different spin-diffusion lengths in the normal metals (λ_i) or different conductances (Re$g^{\uparrow\downarrow}$). For example, taking identical normal metals but different contacts, e.g., a clean and a dirty one, $\Delta\mu_0^{(1)}$ and $\Delta\mu_0^{(2)}$ will be different due to different spin-mixing conductances.

In conclusion, we report a unified description for spin pumping in $F|N$ structure and analyze the spin accumulation in the normal metal induced by a spin-pumping current. We predict generation of a dc voltage over a single $F|N$ junction. The Py|Al system should be an ideal candidate to electrically detect magnetization dynamics in this way. An experimental test of our predictions is in progress [8].

We thank Yu. Nazarov and A. Kovalev for discussions. This work is supported by NanoNed, EU Commission FP6 Projects No. 05587-1 "SFINX" and No. 033749 "DynaMax," and the Research Council of Norway through Grant No. 162742/V00.

[1] Y. Tserkovnyak, A. Brataas, and G. E. W. Bauer, Phys. Rev. Lett. **88**, 117601 (2002).
[2] Y. Tserkovnyak, A. Brataas, G. E. W. Bauer, and B. Halperin, Rev. Mod. Phys. **77**, 1375 (2005).
[3] A. Brataas, Y. Tserkovnyak, G. E. W. Bauer, and B. I. Halperin, Phys. Rev. B **66**, 060404 (2002).
[4] S. M. Watts, J. Grollier, C. H. van der Wal, and B. J. van Wees, Phys. Rev. Lett. **96**, 077201 (2006).
[5] L. Berger, Phys. Rev. B **59**, 11 465 (1999).
[6] J. N. Kupferschmidt, S. Adam, and P. W. Brouwer, cond-mat/0607145.
[7] A. Azevedo, L. H. V. Leao, R. L. Rodriguez-Suarez, A. B. Oliveira, and S. M. Rezende, J. Appl. Phys. **97**, 10C715 (1999); E. Saitoh, M. Ueda, M. Miyajima, and G. Tatara, Appl. Phys. Lett. **88**, 182509 (2006).
[8] M. V. Costache, M. Sladkov, C. H. van der Wal, and B. J. van Wees, following Letter, Phys. Rev. Lett. **97**, 216603 (2006).
[9] A. Brataas, Y. V. Nazarov, and G. E. W. Bauer, Phys. Rev. Lett. **84**, 2481 (2000); Eur. Phys. J. B **22**, 99 (2001).
[10] K. Xia, P. J. Kelly, G. E. W. Bauer, A. Brataas, and I. Turek, Phys. Rev. B **65**, 220401(R) (2002); A. Brataas, G. E. W. Bauer, and P. J. Kelly, Phys. Rep. **427**, 157 (2006).
[11] M. Johnson and R. H. Silsbee, Phys. Rev. B **37**, 5312 (1988).
[12] X. Wang, G. E. W. Bauer, A. Brataas, and Y. Tserkovnyak (unpublished).
[13] Y. Tserkovnyak, A. Brataas, and G. E. W. Bauer, Phys. Rev. B **67**, 140404 (2003).
[14] F. J. Jedema, H. B. Heersche, A. T. Filip, J. J. A. Baselmans, and B. J. van Wees, Nature (London) **416**, 713 (2002); M. Zaffalon and B. J. van Wees, Phys. Rev. Lett. **91**, 186601 (2003).
[15] G. E. W. Bauer, Y. Tserkovnyak, D. Huertas-Hernando, and A. Brataas, Phys. Rev. B **67**, 094421 (2003).
[16] J. Bass and W. P. Pratt, J. Magn. Magn. Mater. **200**, 274 (1999).
[17] A. Fert and L. Piraux, J. Magn. Magn. Mater. **200**, 338 (1999).